ACS Macro Letters

Letter

pubs.acs.org/macroletters

Orientation-Dependent Order−Disorder Transition of Block Copolymer Lamellae in Electric Fields

Heiko G. Schoberth,[†] Christian W. Pester,[†] Markus Ruppel,[§] Volker S. Urban,[⊥] and Alexander Böker*[,†,‡]

[†]Lehrstuhl für Makromolekulare Materialien und Oberflächen, DWI an der RWTH Aachen e.V., RWTH Aachen University, D-52056 Aachen, Germany

[‡]JARA-FIT, RWTH Aachen University, D-52056 Aachen, Germany

[§]Chemical Sciences Division, Oak Ridge National Laboratory (ORNL), Oak Ridge, Tennessee 37831, United States

[⊥]Biology and Soft Matter Division, Oak Ridge National Laboratory (ORNL), Oak Ridge, Tennessee 37831, United States

Supporting Information

ABSTRACT: Electric fields have been shown to stabilize the disordered phase of near-critical block copolymer solutions. Here, we use in situ synchrotron small-angle X-ray scattering to examine how the initial orientation of lamellar domains with respect to the external field (φ) affects the shift in the order−disorder transition temperature (T_{ODT}) of lyotropic solutions of poly(styrene-*b*-isoprene) in toluene. We find a downward shift of the transition temperature, which scales with lamellar orientation as $\Delta T_{ODT} \sim \cos^2 \varphi$, in accordance with theory.

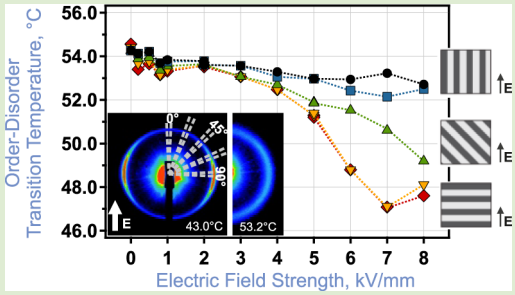

Block copolymers comprise two or more chemically distinct homopolymers covalently linked to each other. These materials have attracted considerable interest due to their ability to readily self-organize into a wide variety of thermotropic and lyotropic mesophases, which paves a powerful path toward the bottom-up fabrication of complex self-assembled geometries on mesoscopic length scales.[1]

To benefit from copolymer-based nanofabrication techniques, numerous methods are widely investigated to afford the deterministic control of block mesophases in bulk and in confined geometries, which are in particular targeted to provide high degrees of translational and orientational order. Examples include temperature and solvent gradients, shear forces, and epitaxial patterning.[2] External electric fields are equally appealing to direct the self-assembly of copolymer mesophases. Promising instances of electric field-induced pattern formation, both in thin films and in bulk, have been reported.[3] Domain alignment,[4−6] structural transitions,[7−9] and thermodynamic properties[10,11] have been studied both experimentally and theoretically and contributed to a profound understanding of the effects of electric fields on block copolymer mesophases.[3,4] Manifold predictions were made regarding the influence of electric fields on the order−disorder transition (ODT) of binary mixtures. Whereas classical thermodynamics predicts phase separation in the presence of an uniform electric field,[11,12] experiments usually unveil the opposite effect, that is, field-induced mixing.[13] Seminal experiments by Debye and Kleboth, who studied the phase behavior of a binary mixture of two solvents, found a decrease of the upper critical solution temperature (UCST) in the presence of a uniform field.[14] Similar results were obtained by Wirtz and Fuller who conducted first experiments involving macromolecules, showing that electric fields lower the UCST of a mixture of polystyrene in cyclohexane by 40 mK.[15] In contrast, the lower critical solution temperature (LCST) of a mixture of poly(*p*-chlorostyrene) in ethylcarbitol was increased by 30 mK under equal experimental conditions, indicating that an electric field indeed favors the disordered phase.[15] In addition, Osuji et al. and Segalman et al. studied the influence of magnetic fields on order−disorder transitions.[16,17] Recently, we investigated the influence of electric fields on concentrated poly(styrene-*b*-isoprene) solutions in toluene, which revealed a suppression of ODT, i.e., a downward shift of the order−disorder transition temperature (T_{ODT}) by 2 K for an electric field of 8.5 kV/mm. This electric field-induced disordering, i.e., the downward shift in T_{ODT}, is expected to scale with the square of the electric field intensity, $\Delta T_{ODT}(E) \sim E^2$, and is believed to naturally depend on the initial domain orientation as interfaces oriented perpendicular to the field direction are rendered thermodynamically unstable.[18] Experimental support, however, is yet pending, which encouraged the present study of the effect of initial domain orientation on the order−disorder transition temperature of a lyotropic block copolymer solution.[10,13,19] The effect of initial lamellar alignment and polymer concentration on the order−disorder transition temperature, T_{ODT}, was investigated by means of in situ synchrotron small-angle X-ray scattering (SAXS). We employed a home-built, temperature-controlled capacitor, which can accommodate

Received: January 8, 2013
Accepted: April 29, 2013
Published: May 14, 2013

square glass capillaries between its electrodes. We used concentrated solutions of a near-symmetrical poly(styrene-*b*-isoprene) diblock in toluene (30.5−35 wt. %). At a total molecular weight of 108 kg/mol, the volume fractions of polystyrene and polyisoprene amounted to 46 and 54 vol. %, respectively ($S_{46}I_{54}^{108}$). Self-assembly above the order−disorder concentration, c_{odc}, forms a lyotropic lamellar phase. Conducting the experiments in solution readily allowed us to circumvent experimental limitations pertinent to high melt viscosities and sample temperatures close to the polymer's decomposition temperature in the solvent-free melt. Heating and cooling cycles at various electric field intensities provided a well-suited method to monitor the effect of an electric field on the phase transition in situ. Prior to each cycle the sample was equilibrated at about 10 K above T_{ODT} and cooled below T_{ODT} in the presence of an electric field of 3 kV/mm and at a rate of −1.25 K/min, resulting in a lamellar morphology with interfaces oriented predominantly parallel to the applied field. Subsequent heating and cooling cycles were conducted to determine the order−disorder transition temperature as a function of the applied field intensity.

SAXS patterns of $S_{46}I_{54}^{108}$ copolymer lamellae exhibit characteristic Bragg diffraction at q_{hkl}/q_{100} = 1:2:3. Here, q denotes the magnitude of the wave vector of the scattered radiation. For lamellae with interfaces parallel to the applied field the scattered intensity accumulates at azimuthal angle φ = 90° (Figure 1a: far left), where φ denotes the angle between the lamellar normal, **n**, and the electric field, **E**.

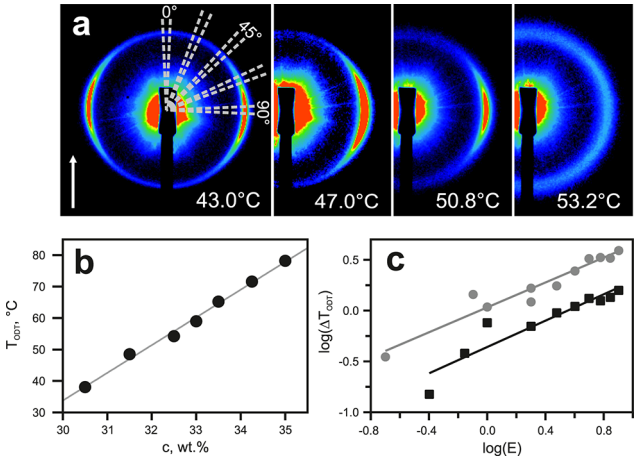

Figure 1. (a) SAXS patterns from a 32.5 wt. % solution of $S_{46}I_{54}^{108}$ in toluene during heating at 1.25 K/min and an electric field of 4.0 kV/mm. The arrow indicates the direction of the applied field. The five analyzed, wedge-shaped sectors with opening angle of $\Delta\varphi$ = 5° are shown for azimuthal angles ranging from φ = (0 ± 2.5)° to φ = (90 ± 2.5)°. (b) The order−disorder scales linearly with polymer concentration. (c) Double-logarithmic plot of the shift in T_{ODT} vs E for solutions of $S_{46}I_{54}^{108}$ in toluene: 30.5 wt. % (bullets) and 32.5 wt. % (squares).

Upon heating poly(styrene-*b*-isoprene) above T_{ODT}, its lamellar microstructure disintegrates, and long-range order fades. This is connected to a significant change in the line shape of the first-order Bragg peak. Lamellar microdomains exhibit multiple, sharp, and well-defined Bragg peaks at defined ratios (Figure 1a: far left). In contrast, peak properties in the disordered state are governed by a suppression of the forward scattering contribution, owing to the linkage between chemically distinct diblock components; i.e., a correlation hole exists at small scattering angles. Consequently, the maximum peak intensity, $I_{max}(q)$, is of a substantially lower magnitude, exhibiting a considerably increased peak width, i.e. full-width at half-maximum (fwhm), and a Lorentzian line shape[20] for temperatures above T_{ODT} (Figure 1a: far right).[21] For experiments presented here, the discontinuities of both fwhm and $I_{max}(q)$ together with a close observation of the first-order Bragg peak's line shape were used to determine T_{ODT}.

Figure 2a illustrates the temperature evolution of the Bragg peak characteristics for the 2D scattering patterns depicted in

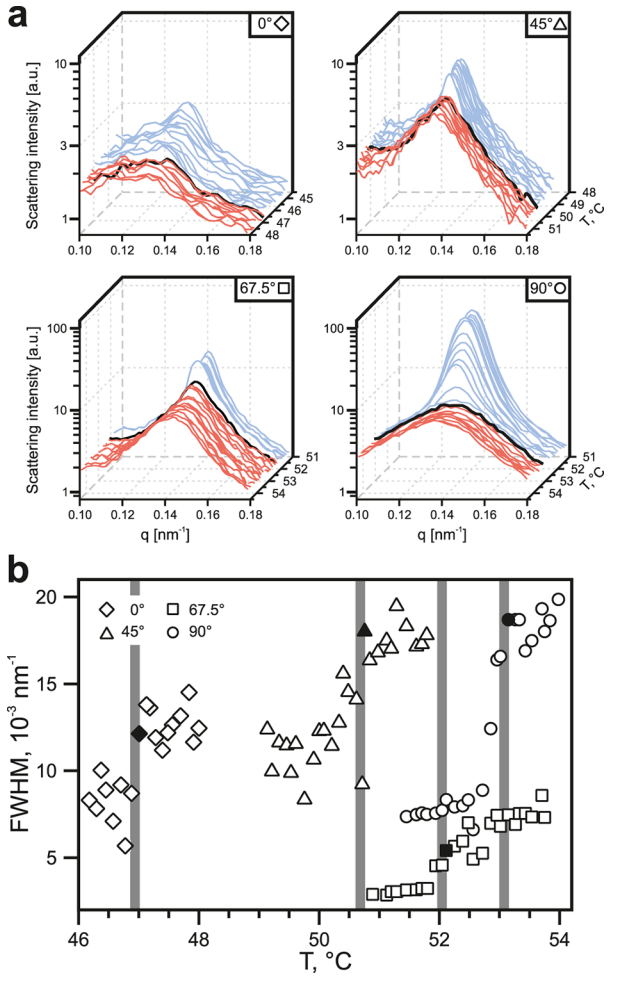

Figure 2. (a) Time evolution of the first-order Bragg peak for individual φ-sectors for a 32.5 wt. % solution of $S_{46}I_{54}^{108}$ at 7.0 kV/mm. (b) Determination of T_{ODT} from the discontinuity of the first-order Bragg peak's fwhm. Black curves in (a) correspond to the full symbols in (b), which mark the transition point, further indicated by dark gray lines. Please note that for clarity reasons data for φ = 67.5° (squares) were shifted downward by 3 × 10^{-3} nm^{-1}.

Figure 1a. Artifacts from domain reorientation can be excluded by evaluating the peak width, which relates to the thermodynamic stability of the microphase.

Figure 1b displays the transition temperatures for various concentrations in the absence of an external field. A linear relation between T_{ODT} and polymer concentration is obtained in accordance with the dilution approximation.[22−24] Extrapolation to room temperature yields the order−disorder concentration, c_{odc} = 28.5 wt. %, in excellent agreement with an independent determination under ambient conditions (c_{odc}

dx.doi.org/10.1021/mz400013u | *ACS Macro Lett.* 2013, 2, 469−473

= 28.3 wt. %). The shift of the transition temperature, $\Delta T^{E}_{ODT} = T_{ODT}(E = 0) - T_{ODT}(E)$, as a function of applied field strength is demonstrated in Figure 1c. T_{ODT} generally decreases by approximately 1.0 K for $E < 4$ kV/mm, while a suppression by 1.5 K is obtained for higher fields. Power-law analysis indicates an apparent scaling, as $\Delta T_{ODT}(E) \sim E^{\alpha}$ with the exponent $\alpha = 0.65 \pm 0.09$ for the 32.5 wt. % solution from Figure 1a. This exponent was confirmed for an additional 30.5 wt. % solution, $\alpha = 0.61 \pm 0.05$.

This stands in marked contrast to basic electrostatic considerations pertaining to the Gibbs energy of a multicomponent mixture in the presence of an applied field, which predicts a quadratic scaling with E.[25−27] Onuki predicts a weaker field dependence in the limit of strong fields scaling as, $\Delta T_{ODT} \sim E^{1.6}$,[26] which may well be pertinent to our experiments, considering that fields applied in this study were at least an order of magnitude stronger than the crossover field considered by Onuki.[13] Further deviation from the $\sim E^2$ scaling may arise from a nonlinear behavior of the dielectric permittivity as evident for dielectric mixtures in close vicinity to ODT.[26,28] Yet, both effects are deemed insufficient to reasonably account for observed scaling, and we can thus only speculate on its cause. This may include layers of lamellae being absorbed on the glass surface of the capillaries used to accommodate the polymer solutions.[29] Considering an absorption layer, for which the thickness depends on the applied field, its polarization (which scales linearly with E) would imply a field-dependent screening of the external field. Polarization effects and generally weaker field dependence as predicted in the limit of strong fields may thus indeed account for apparent scaling.

In the remainder of this article, we focus on the effect of initial lamellar alignment on T_{ODT}. Although we present only data for a 32.5 wt. % solution of $S_{46}I_{54}$[108] in toluene, all investigated concentrations show similar trends (refer to Supporting Information). Figure 2a depicts the temperature evolution of the first-order Bragg peak for four of the five wedge-shaped sectors of $\Delta\varphi = 5°$ opening angle (cf. Figure 1a, far left image). Sector orientation corresponds to the orientation of the lamellar normal with respect to the electric field vector, **E**. Upon disordering, intensity bleeds into a correlation hole, and the intensities of all sectors decrease. Figure 2b shows the accompanied discontinuity of the first-order Bragg peak's fwhm, which was used to determine transition temperatures. Representative field-dependent transition temperatures for various sector orientations are plotted in Figure 3a. T_{ODT} is generally lowered with increasing field strength and depends considerably on lamellar orientation. Lamellae with interfaces oriented parallel to the applied field ($\varphi = 90°$) exhibit the weakest response as compared to lamellae with perpendicular orientation ($\varphi = 0°$). The orientation-dependent shift in T_{ODT} amounts to about 0.5 and 5 K for lamellae oriented parallel and perpendicular to a field of 8 kV/mm, i.e., lamellae oriented perpendicular to **E** disorder at lower temperatures than lamellae with parallel orientation.

Solutions were studied for various polymer concentrations above the order-disorder concentration. Data is provided as Supporting Information and shows how the influence of the electric field on T_{ODT} becomes more significant with increasing concentration. The overall transition temperature (averaged over all azimuthal orientations) coincides with the disordering of the most stable lamellar orientation with interfaces parallel to **E**, $T^{\parallel}_{ODT}$. Amundson et al. derived a Landau free energy

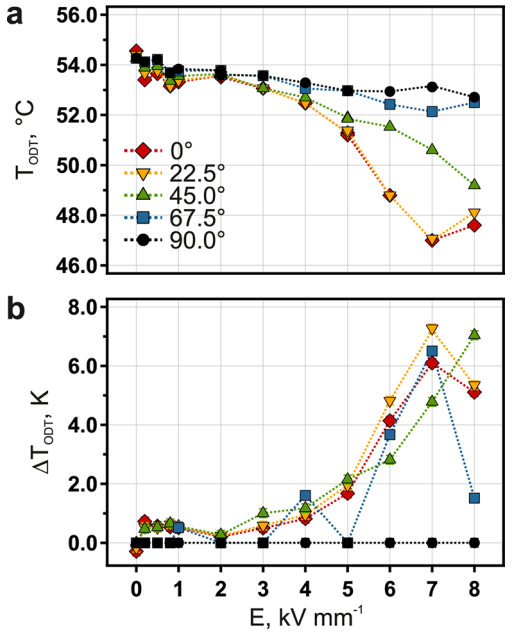

Figure 3. (a) Determination of the influence of the electric field on T_{ODT} for individual φ-sectors for a 32.5 wt. % solution of $S_{46}I_{54}$[108] in toluene. (b) Orientation-dependent shift of ΔT_{ODT} vs electric field strength, E, with normalization according to $\Delta T_{ODT}(\varphi) = \Delta T^{\varphi}_{ODT}(\varphi)/\cos^2\varphi$.

functional for modulated block copolymer phases in the weak-segregation limit in proximity to ODT, which implies an energy penalty for ill-aligned lamellae ($\varphi \neq 90°$). Accordingly, lamellar interfaces perpendicular to the external field will be the first to be destabilized. The cause is founded in the polarization of interfaces between chemically distinct domains, which differ in dielectric permittivity. This adds an additional electric energy contribution due to the excess dielectric displacement at the interfaces of ill-aligned lamellae. Consequently, the interaction parameter at the transition is shifted by $\chi_t N = \chi_s N + k_1 \cdot N^{-1/3} + k_2 \cdot \eta_{elec}$, with numerical constants k_1 and k_2, the number of repeating units, N, and the electric field energy density, η_{elec}.[6]

As mentioned above, we initially rescaled our data to account for electric field-induced shifts in T_{ODT} according to $\Delta T^{E}_{ODT} = T_{ODT}(E = 0) - T_{ODT}(E)$. The electric field energy density, η_{elec}, scales with the square cosine of the angle between lamellae normal, **n**, and electric field vector, **E**, as $\eta_{elec} \sim \cos^2\varphi \cdot E^2$. The difference in χN, i.e., the difference of $T_{ODT}(E)$ between domains oriented at angles φ_1 and φ_2, can be determined by[6]

$$\Delta\chi N = \chi N(\varphi_1) - \chi N(\varphi_2) \cong [\cos^2(\varphi_1) - \cos^2(\varphi_2)]E^2 \quad (1)$$

For the thermodynamically most stable, parallel lamellae ($\varphi_1 = 90°$) the first term of this expression vanishes. To compare the stability of further orientations, rescaling of all sector data according to $\Delta T^{\varphi}_{ODT} = \Delta T^{E}_{ODT}(\varphi) - \Delta T^{E}_{ODT}(\varphi = 90°)$ was performed. The energetic penalty increases with $\cos^2\varphi$, and hence subsequent normalization of $\Delta T^{\varphi}_{ODT}(\varphi)$ by $\cos^2\varphi$ as $\Delta T_{ODT}(\varphi) = \Delta T^{\varphi}_{ODT}(\varphi)/\cos^2\varphi$ should create an orientation-independent master curve. In coherence with Amundson's predictions, Figure 2 demonstrates how all sector data indeed coincide irrespective of domain orientation within experimental errors. Deviations apparent for small angles can be attributed to uncertainties in determining $\Delta T_{ODT}(\varphi)$ for the smallest tilting angles.

dx.doi.org/10.1021/mz400013u | ACS Macro Lett. 2013, 2, 469−473

To conclude, we studied the influence of the initial lamellar orientation on the electric field-induced order−disorder transition for concentrated solutions of poly(styrene$_{46}$-*b*-isoprene$_{54}$)^{108} in toluene. The order-disorder transition temperature is generally lowered in the presence of an applied field. The shift of the transition temperature $\Delta T_{ODT}(E)$ with increasing field strength depends strongly on polymer concentration and initial lamellar orientation, i.e., lamellae oriented perpendicular to the field disorder at considerably lower temperatures as parallel oriented ones. The orientation-dependent shift $\Delta T_{ODT}(E, \varphi)$ increases with φ, and data suggest $\Delta T_{ODT}(E, \varphi) \sim \cos^2 \varphi$ within experimental errors—in accordance with theory.

MATERIALS AND METHODS

Lamellae forming poly(styrene-*b*-isoprene) diblock copolymer ($S_{46}I_{54}^{108}$) was synthesized via sequential living anionic polymerization.[30] $S_{46}I_{54}^{108}$ consists of 46 wt. % polystyrene and 54 wt. % polyisoprene as determined by NMR. Molecular weight (M_n = 108 kg/mol) and polydispersity (M_w/M_n = 1.05) were determined by GPC. The polymer was dissolved in toluene with concentrations ranging from 30.5 to 35.0 wt. %. Temperature-controlled experiments were performed in a home-built cubic capacitor designed to accommodate flame-sealed square 2 × 2 mm^2 glass capillaries between its gold electrodes. The entire capacitor was immersed in insulating oil, which afforded precise control over sample temperature with accuracy greater than ±0.05 K. A dc voltage of up to 16 kV was applied, resulting in a homogeneous external electric field of up to 8 kV/mm. Synchrotron SAXS was conducted at the ID02 beamline at the European Synchrotron Radiation Facility (ESRF, Grenoble, France). The beam size at sample position was 150 × 300 μm (vertical × horizontal) at a photon energy of 12 keV. SAXS patterns were recorded with a Kodak FreLoN CCD detector at a sample−detector distance of 5 m. Prior to data analysis, data were corrected for detector efficiency and geometry and normalized to transmitted intensity. Next we determined the transition temperature (T_{ODT}). As the volume of the capillaries is small compared to the volume of the surrounding oil bath, the bath temperature was taken as the sample temperature. A constant heating rate of 1.25 K/min was applied to heat the sample above T_{ODT}. This heating rate is sufficiently slow not to compromise individual transition temperatures and forms a compromise between reproducible values and short experimental duration required due to limited beamtime. The sample was allowed to equilibrate in the disordered state for several minutes, before it was cooled below T_{ODT} at the same rate. At a constant temperature in the ordered (lamellar) state an electric field of 3 kV/mm was applied to orient the lamellae parallel to the applied field and ensure equal starting conditions prior to individual successive temperature cycles.[31] Subsequently, the transition temperature was determined in the presence of an electric field of various strength upon heating the sample into the disordered state by evaluating the discontinuity of the first-order Bragg peak's full width at half-maximum (fwhm) and peak shape. The field was applied in a random sequence in an attempt to avoid systematic errors.

ASSOCIATED CONTENT

Supporting Information

Additional data for different concentrations of materials. This material is available free of charge via the Internet at http://pubs.acs.org.

AUTHOR INFORMATION

Corresponding Author

*E-mail: boeker@dwi.rwth-aachen.de.

Author Contributions

Heiko G. Schoberth and Christian W. Pester contributed equally. The manuscript was written through contributions of all authors. All authors have given approval to the final version of the manuscript.

Notes

The authors declare no competing financial interest.

ACKNOWLEDGMENTS

H.G.S., C.W.P., and A.B. thank the European Union and the German Science Foundation (DFG, BO 2475/5−1) for financial support in the framework of the ERA-NanoSci+ project MEMORY. M.R. and V.S.U. were supported by the U.S. Department of Energy, Basic Energy Sciences, Materials Sciences and Engineering Division. The authors thank P. Boesecke, T. Narayanan, M. Sztucki, and E. di Cola for their help at the ESRF and F. Fischer, H. Zettl, and H. Krejtschi and his team for assistance with building the capacitors. We are grateful to the ESRF for provision of synchrotron beam time and thank K. A. Schindler, K. Schmidt, S. Hüttner, C. Liedel, and A. Mihut for assistance during the measurements.

REFERENCES

(1) Ball, P. *Nature* **2001**, *413*, 667.
(2) Sakurai, S. *Polymer* **2008**, *49*, 2781−2796.
(3) Liedel, C.; Pester, C. W.; Ruppel, M.; Urban, V. S.; Böker, A. *Macromol. Chem. Phys.* **2012**, *213*, 259−269.
(4) Amundson, K.; Helfand, E.; Davis, D. D.; Quan, X.; Patel, S. S.; Smith, S. D. *Macromolecules* **1991**, *24*, 6546−6548.
(5) Amundson, K.; Helfand, E.; Quan, X.; Smith, S. D. *Macromolecules* **1993**, *26*, 2698−2703.
(6) Amundson, K.; Helfand, E.; Quan, X.; Hudson, S. D.; Smith, S. D. *Macromolecules* **1994**, *27*, 6559−6570.
(7) Schmidt, K.; Schoberth, H. G.; Ruppel, M.; Zettl, H.; Hänsel, H.; Weiss, T. M.; Urban, V. S.; Krausch, G.; Böker, A. *Nat. Mater.* **2008**, *7*, 142−145.
(8) Pester, C. W.; Ruppel, M.; Schoberth, H. G.; Schmidt, K.; Liedel, C.; Van Rijn, P.; Schindler, K. A.; Hiltl, S.; Czubak, T.; Mays, J.; Urban, V. S.; Böker, A. *Adv. Mater.* **2011**, *23*, 4047−4052.
(9) Schmidt, K.; Pester, C. W.; Schoberth, H. G.; Zettl, H.; Schindler, K. A.; Böker, A. *Macromolecules* **2010**, *43*, 4268−4274.
(10) Gunkel, I.; Stepanow, S.; Thurn-Albrecht, T.; Trimper, S. *Macromolecules* **2007**, *40*, 2186−2191.
(11) Schoberth, H. G.; Schmidt, K.; Schindler, K. A.; Böker, A. *Macromolecules* **2009**, *42*, 3433−3436.
(12) Tsori, Y.; Tournilhac, F.; Leibler, L.; Ho, F. *Nature* **2004**, *430*, 544−547.
(13) Orzechowski, K. In *Polymers, Liquids and Colloids in Electric Fields: Interfacial Instabilites, Orientation and Phase Transitions.* Tsori, Y., Steiner, U., Eds.; World Scientific Publishing Company: New Jersey, 2009, pp 87−112.
(14) Debye, P.; Kleboth, K. *J. Chem. Phys.* **1965**, *42*, 3155−3162.
(15) Wirtz, D.; Fuller, G. G. *Phys. Rev. Lett.* **1993**, *71*, 2236−2239.
(16) Gopinadhan, M.; Majewski, P. W.; Choo, Y.; Osuji, C. O. *Phys. Rev. Lett.* **2013**, *110*, 078301.
(17) Mcculloch, B.; Portale, G.; Bras, W.; Segalman, R. A. *Macromolecules* **2011**, *44*, 7503−7507.
(18) Onuki, A. *Phys. A* **1995**, *217*, 38−52.
(19) Debye, P.; Kleboth, K. *J. Chem. Phys.* **1965**, *42*, 3155−3162.
(20) Sakamoto, N.; Hashimoto, T. *Macromolecules* **1995**, *28*, 6825−6834.
(21) Leibler, L. *Macromolecules* **1980**, *13*, 1602−1617.
(22) Helfand, E. *J. Chem. Phys.* **1972**, *56*, 3592.
(23) Lodge, T. P.; Pan, C.; Jin, X.; Liu, Z.; Zhao, J.; Maurer, W. W.; Bates, F. S. *J. Polym. Sci., Part B: Polym. Phys.* **1995**, *33*, 2289−2293.
(24) Hanley, K. J.; Lodge, T. P. *J. Polym. Sci., Part B: Polym. Phys.* **1998**, *36*, 3101−3113.
(25) Landau, L. D.; Lifshitz, E. M.; Pitaevskii, L. P. *Electrodynamics of Continuous Media*; Elsevier Butterworth-Heinemann, 2004.

(26) Rzoska, S. J.; Zhelezny, V. *Nonlinear dielectric phenomena in complex liquids*; Kluwer Academic Publishers: Dordrecht, 2004.
(27) Tsori, Y.; Steiner, U. *Polymers, Liquids and Colloids in Electric Fields*; World Scientific Publishing Co. Pte. Ltd.: Singapore, 2009.
(28) Orzechowski, K. *Chem. Phys.* **1999**, *240*, 275−281.
(29) Tsori, Y.; Andelman, D. *Macromolecules* **2002**, *35*, 5161−5170.
(30) Baskaran, D.; Müller, A. H. E. In *Controlled and Living Polymerizations: From Mechanisms to Applications*; Müller, A. H. E., Matyjaszewski, K., Eds.; Wiley-VCH: Weinheim, 2009.
(31) Böker, A.; Knoll, A.; Elbs, H.; Abetz, V.; Müller, A. H. E.; Krausch, G. *Macromolecules* **2002**, *35*, 1319−1325.